Application note

Evaluating Silicon using Raman Microscopy

Authors

Robert Heintz & Alexander Rzhevskii

Industry/Application:
Semiconductor, microelectronics, lithium-ion batteries, aluminum manufacturing

Products used:
Thermo Scientific™ DXR3 Raman Microscope

Thermo Scientific™ DXR3xi Raman Imaging Microscope

Goals:
Demonstrate the range of information provided from the Raman analysis of silicon in different applications.

Key Analytes:
Silicon, aluminum alloys, nano-scaled silicon powder, nickel silicides, semiconductor nanomembranes

Key Benefits:
Raman imaging provides molecular and chemical views of silicon materials based on the spatial distribution of components or on differences in physical states that are essential for evaluating the properties of those materials.

Significance

Silicon is a vital technological material that is used in numerous different types of applications. Proper evaluation of the properties of the silicon or silicon-containing materials is essential to ensure the materials are appropriate for their intended use. The analyses of different types of silicon samples by means of Raman microscopy are presented here to illustrate the information that can be garnered from Raman analysis, including identification of components, evaluation of morphology, and visualization of mechanical strain. The physical state of silicon is key to determining its properties and effectiveness for different applications, including use in solid state electronics, in materials to improve battery capacity, and in alloys with improved castability and strength. This review is not intended to be all-inclusive of everything that can be done with Raman spectroscopy in terms of the analysis of silicon materials, but to show a few examples of what is possible.

Introduction

Raman spectroscopy is a form of vibrational spectroscopy that probes chemical bonds and molecular structure and is sensitive to small changes in chemical and structural environments. The Raman spectrum of a material is a molecular "fingerprint" that can be used for identification of unknown materials and for characterizing and qualifying expected materials. Since intermolecular effects and lattice vibrations are also detected, it can be used to evaluate crystallinity. Mechanical phenomena such as strain can also be detected from peak shifts in Raman spectra. Raman imaging allows visualization of the distribution of components or changes in physical state across the sample.

Silicon in aluminum

Silicon is used in alloys with aluminum to increase the strength of lightweight aluminum-based parts. Addition of silicon to aluminum also alters the viscosity of melted aluminum, improving the castability. These alloys typically contain 3% to 25% silicon. While silicon and aluminum can form a eutectic mixture, it is common to have finely dispersed silicon particles throughout the material.[1] The size and distribution of silicon particles can affect the strength of the aluminum.

One common example of an aluminum product, aluminum foil, is made up of almost pure aluminum (approximately 98.5%) but it does contain small amounts of silicon and iron.[2] Raman imaging of a piece of aluminum foil reveals small particles of silicon (Figure 1). A Thermo Scientific™ DXR3xi Raman Imaging Microscope was used with a 532 nm laser and a 100X metallurgical objective to collect the Raman imaging data. An area of 408 µm x 208 µm was imaged using an image pixel size of 1 µm. The Raman image, based on the 520 cm^{-1} peak of silicon, shows the spatial distribution of the particles and image analysis provides size and shape information. In this case, 81 silicon particles were identified with a size (area) range of 6-151 $µm^2$. This analytical approach may be extrapolated to other types of Si/Al alloy parts.

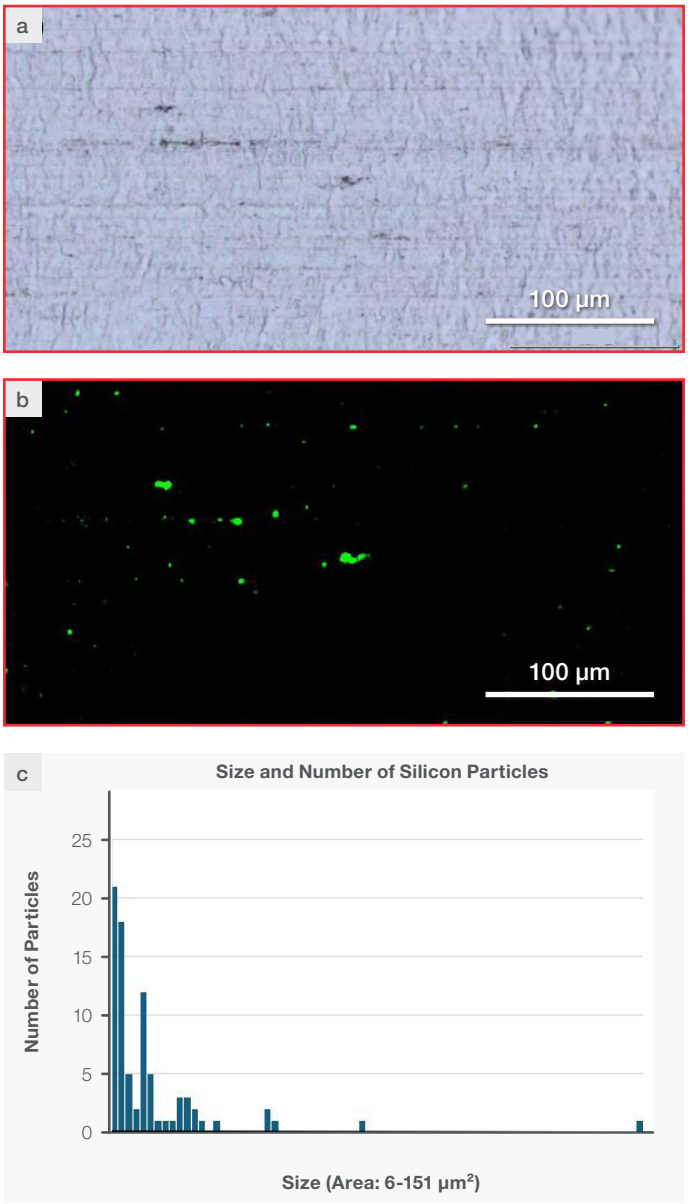

Figure 1. (a) Visual mosaic image of the aluminum foil sample (100x objective). (b) Raman image based on the peak area of the 520 cm^{-1} peak of silicon (green indicates silicon particles). (c) Distribution of aluminum particle sizes from image analysis of the Raman peak area image.

Silicon anodes

Graphite is a common anode material in lithium-ion batteries due to its low cost and good reversible intercalation of lithium. However, graphite is limited in its theoretical capacity (372 mAh/g),[3] and higher capacity is a key factor for improving battery performance. Silicon-based anode materials are attractive because of the high theoretical specific capacity (3579 mAh/g) of silicon.[4] The issue with using silicon is that the intercalation of lithium is accompanied by a very large change in volume, and with repeated charge and discharge cycles, the vacillating expansion and contraction causes cracking and pulverization of the anode material, which results in mechanical degradation, increased resistance, and a reduced capacity. There have been many approaches to circumventing this volume expansion problem including, but not limited to, use of nanoparticles of silicon, use of materials with porous silicon structures, and incorporation of carbon-silicon composite materials. It is reported that particles of silicon having diameters below 150 µm can accommodate the volume expansion without fracturing.[3]

It is important to have a way to evaluate the morphology of a silicon material to determine its suitability for use in silicon anodes. The Raman peak of silicon broadens and shifts to shorter wavelengths when going from bulk crystalline silicon to nano-structured silicon particles. This is related to the long-range order (crystallinity) of the silicon, which decreases with the decrease in particle size. Raman imaging provides a way of checking on the homogeneity and spatial distribution of silicon particles with different crystalline domains and particle sizes.

A Raman images of a nano-scaled silicon powder is shown in Figure 2b. The sample was spread out on a microscope slide for analysis. The Raman imaging data and visual image (Figure 2a) were collected using a DXR3xi Raman Imaging Microscope with a 50X metallurgical objective. The area analyzed was 433 µm x 400 µm with an image pixel size of 1 µm. A 455 nm laser was used with a laser power of 1.0 mW to avoid any laser-induced changes in the particles. The Raman image (Figure 2b) is based on multivariate curve resolution (MCR) processing of the Raman spectra and the different colored components represent silicon peaks with different shifts and peak widths (see Figure 2c). In Figure 2c, the Raman spectrum from a silicon wafer was added as a reference and the other three spectra are representative of spectra from the different colored areas (red, blue, and green) in Figure 2b. There is a shift to lower frequencies and a broadening of the peaks going from red to blue to green indicating a decrease in crystallinity and presumably smaller silicon particles. This approach can be used to evaluate silicon anode materials and observe any changes in silicon anodes.

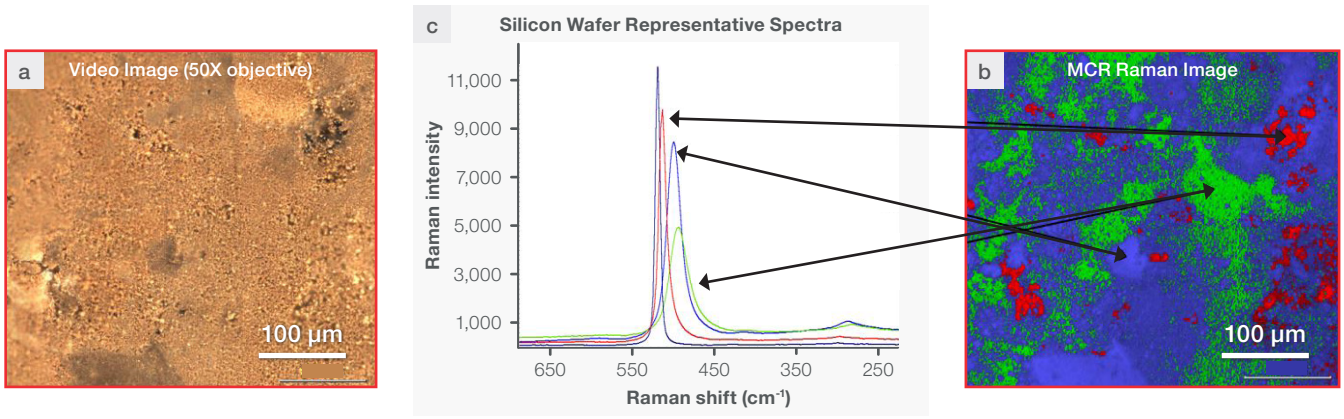

Figure 2. (a) Video mosaic image of the silicon anode powder on a microscope slide. (b) Multivariate curve resolution Raman image where the colors represent silicon peaks with different shifts and peak widths. (c) Representative spectra from the Raman image.

Nickel silicide (NiSi) thin films

Raman microscopy is currently one of the preferred methods for analyzing semiconductor interfaces, microstructures, and devices. The properties of such structured materials can be highly dependent on microscopic-scale inhomogeneities and their spatial distributions.

The following example illustrates the Raman microscopic characterization of nickel silicide (NiSi) thin films that are extensively used for the formation of local metal-semiconductor junctions in metal oxide semiconductors (MOS) and photovoltaic cells. The Raman images were acquired using a Thermo Scientific™ DXR3 Raman Microscope with 532 nm excitation and 5 µm sampling steps (1406 spectra in all). Figure 3 shows the optical image (a), Raman images (b, c) and Raman spectra (d) obtained from a die on Si wafer after thermal processing of Ni thin films deposited on the substrate. The optical and spectral acquisitions were made using a 100x metallurgical objective having a 0.9 numerical aperture. The Raman image in Figure 3b was generated as a sum of integrated intensities (areas) of the spectral bands at 362, 290, 215 and 196 cm^{-1} assigned to monosilicide phase, NiSi,[5] and the image in Figure 3c was constructed as the integrated intensity of the weaker spectral band at 109 cm^{-1}. Representative Raman spectra from the locations indicated by the arrows in Figures 3b and 3c are shown in Figure 3d. The minor Raman band at 109 cm^{-1} and the appearance of the band at 310 cm^{-1} are consistent with the Ni_2Si phase and it may be present in the NiSi alloy despite the increased silicidation temperature. The results illustrate how Raman images are used to evaluate the homogeneity of the coverage of the monosilicide NiSi across the surface along with showing the spatial distribution of the residual Ni_2Si.

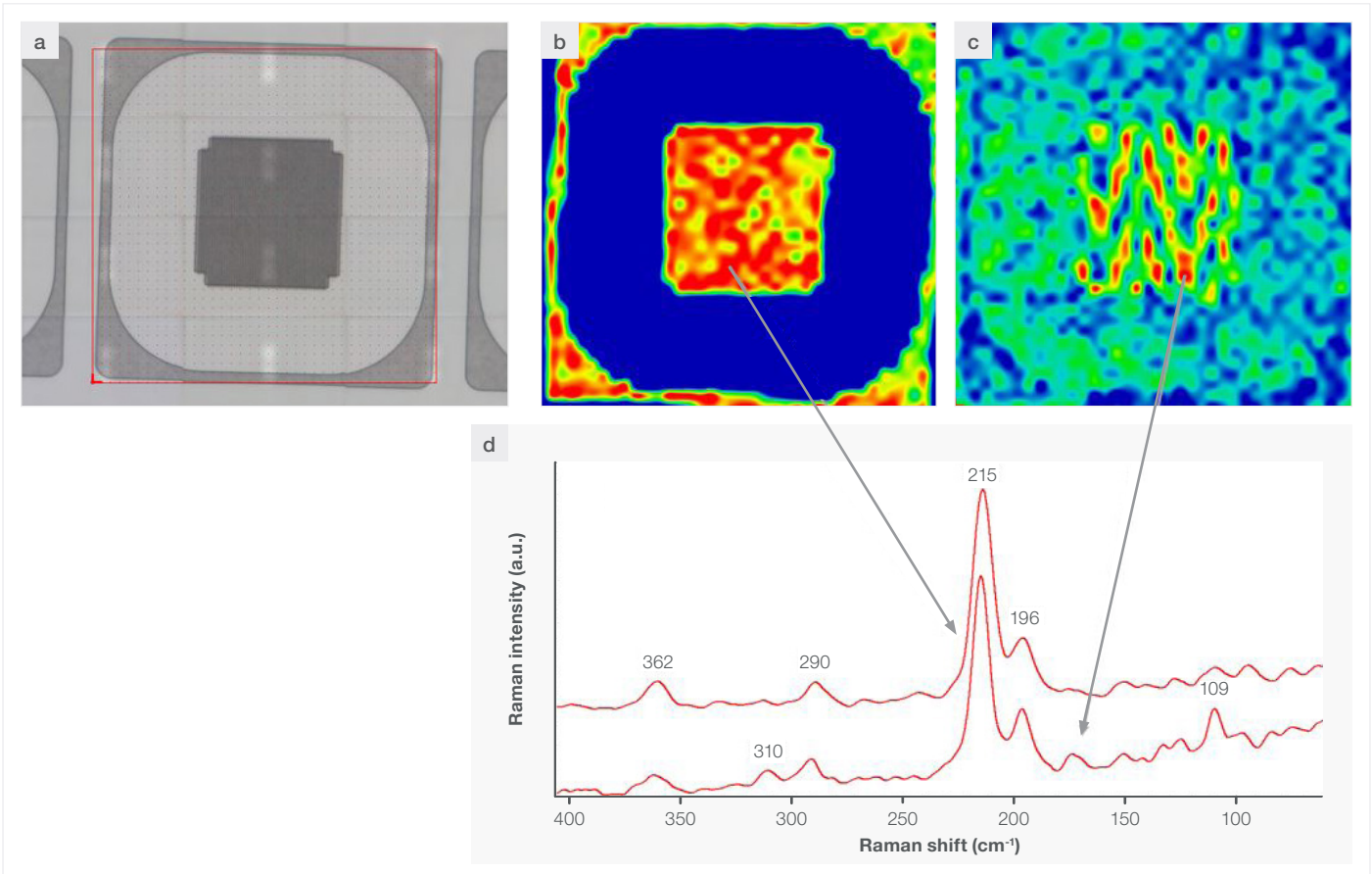

Figure 3. (a) Visual image of a die on silicon wafer after thermal processing of Ni thin films deposited on the substrate and (b) and (c) the Raman images of the die. (d) The representative Raman spectra from selected locations in the images pointed by the arrows.

Silicon nanoribbons

The properties of silicon make it a very important semiconducting material, but in terms of mechanical properties, bulk crystalline silicon is stiff and brittle. One technological area of interest is the push toward flexible and stretchable electronic and optoelectronic materials for use in things like flexible displays, thin film transistors, sensors, and flexible solar cells. One approach is to make composite materials involving a semiconductor nanomembrane supported on a flexible, stretchable substrate. Silicon nanomembranes with thickness less than 500 nm are flexible while maintaining their electronic and optical properties[6] while the elastic modulus of the supporting substrate dominates the mechanical properties.[7] The samples shown in this report are 220 nm thick silicon nanoribbons supported on a polydimethylsiloxane (PDMS) substrate.[8] The PDMS substrate was treated to have a pattern of active sites (hydrophilic Si-OH) sites) on it that bond to the silicon nanoribbons but only at those particular sites. The PDMS substrate swells when treated with a solvent and then contracts when the solvent evaporates in air. When the silicon ribbons are transferred to the PDMS they bind to the active sites and when the substrate shrinks the areas that are not tethered to the substrate buckle.

A portion of the silicon ribbon sample was analyzed with a DXR3xi Raman Imaging Microscope configured with a 455 nm laser and a 100x metallurgical objective in 3-D confocal Raman imaging mode. A total volume of 42.5 µm x 237.0 µm x 34 µm was imaged using a 0.5 µm image pixel size.

In this setup, the 3-D Raman image may be generated to display specific attributes of the Raman spectra (peak intensities, peak positions, spectral correlations, etc.) within the volume. Figure 4 shows a visual image (4a) of the sample as well as 3 different views of the silicon ribbon based on different aspects of the Raman spectra (4b-d). The image in Figure 4b is based on the intensity of the silicon peak and shows the size and shape of the Si ribbon. The image in Figure 4c is based on the position of the silicon peak, which shifts (see Figure 4e) when silicon is strained. More details on the evaluation of strain in silicon will be addressed in the next section. The peak position for silicon in the blue area is typical of unstrained silicon and the peak position for silicon in the red area is shifted to higher frequencies indicating compressive strain. The image based on the correlation to a standard silicon spectrum (4d) showed the presence of a fluorescing contaminant (blue spectrum in Figure 4f and blue area in Figure 4d) on the ribbon. While this does not identify the contaminant, it does locate it. Similar profiles could be used to image the PDMS support but those have not been included here. This example shows how Raman imaging can be used to gather different types of information from these types of samples.

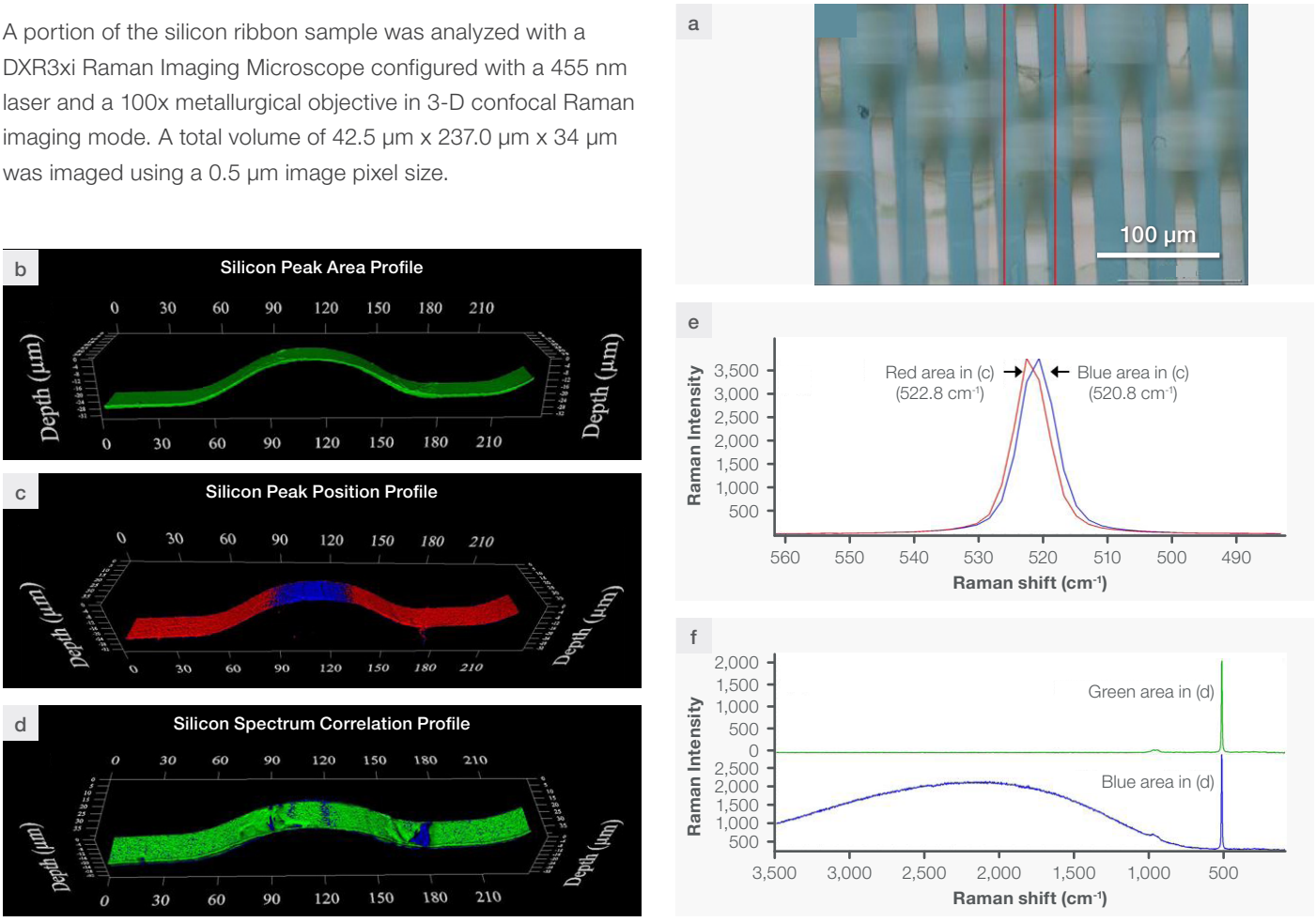

Figure 4. (a) Visual mosaic image of silicon nanoribbons on PDMS. The red box indicates the area imaged. (b) 3-D image of a silicon nanoribbon based on the peak area of the main silicon peak. (c) Raman image based on a silicon peak position profile (blue is unstrained silicon and red is strained silicon). (d) Raman image based on a correlation to a typical silicon spectrum (green area is typical silicon and blue area is fluorescence impurity). (e) Representative spectra showing the shift (strain) in the Raman spectra from 4c. (f) Representative spectra from 4d showing the fluorescence.

Stress-induced strain in silicon

Stress is a concern in microelectronic circuit production. The production of integrated circuits (IC) involves many steps including different types of treatments as well as the formation of embedded microstructures which involves depositing materials with different crystal lattices and thermal expansion coefficients. These processing steps can result in the development of stresses leading to strain in the materials. Strain in semiconductors leads to changes in optical and electronic properties such as changes in non-linear optical phenomena, band gaps, and carrier mobility. Mechanical strain also affects the nucleation and propagation of dislocations as well as the formation of cracks and voids.[9] While strain can be detrimental, in some cases, strain is engineered into materials to dial in and select specific properties.[10] Whether trying to avoid the adverse effects of unwanted stress, or working to use stress to produce desired properties, it is important to be able to evaluate and control the stress so as to produce reliable devices.

Raman microscopy has been extensively used to observe and study the effects of stress in semi-conductor materials.[9,11] The resonant frequencies of the molecular lattice vibrations change with strain and as a result there is a shift in the position of the associated Raman peaks relative to the strain-free state of the material. The extent of the shift is related to magnitude of the strain. The direction of the shift corresponds to the type of stress in which compressive stress leads to an increase of the Raman scattering frequency while tensile stress leads to its decrease.

The sample shown in Figure 5a is a layered semiconductor nanomembrane consisting of a 41 nm thick $Si_{0.704}Ge_{0.296}$ layer deposited on a silicon substrate and then capped with a 23 nm thick epilayer of silicon.[12] The lattice mismatch between the Si-Ge layer and the silicon layers results in stress and strain in the sample. As part of the sample processing, the semiconducting nanomembrane would eventually be completely freed from the silicon substrate, but in this case the semiconductor nanomembrane is not fully released yet and this causes the wrinkles observed in the sample. The dark circle in the center of the wrinkles is a hole in the semiconductor nanomembrane that gives access to the silicon substrate and is part of the process to release the nanomembrane. A 62.5 µm x 67.9 µm area was imaged using a DXR3xi Raman Imaging Microscope configured with a 455 nm laser. The laser power was lowered to 1 mW to avoid any potential heating of the sample. A 100x metallurgical objective was used and spectra were collected using an image pixel size of 0.1 µm. The Raman image in Figure 5b is based on the position of the silicon peak from either the epilayer or the substrate with the colors indicating shifts in the peak position from white (520.7 cm^{-1}) to black (512.4 cm^{-1}). The white circle in the center of Figure 5b is the silicon substrate and hence the spectrum does not show the Si peak from the Si-Ge layer. The other spectra show both the Si peak from the epilayer and the Si peak from the Si-Ge layer. Figure 5c shows representative spectra from the colored areas in the image. This provides a way to visualize the strain in the sample resulting from the stress imposed by the lattice mismatch.

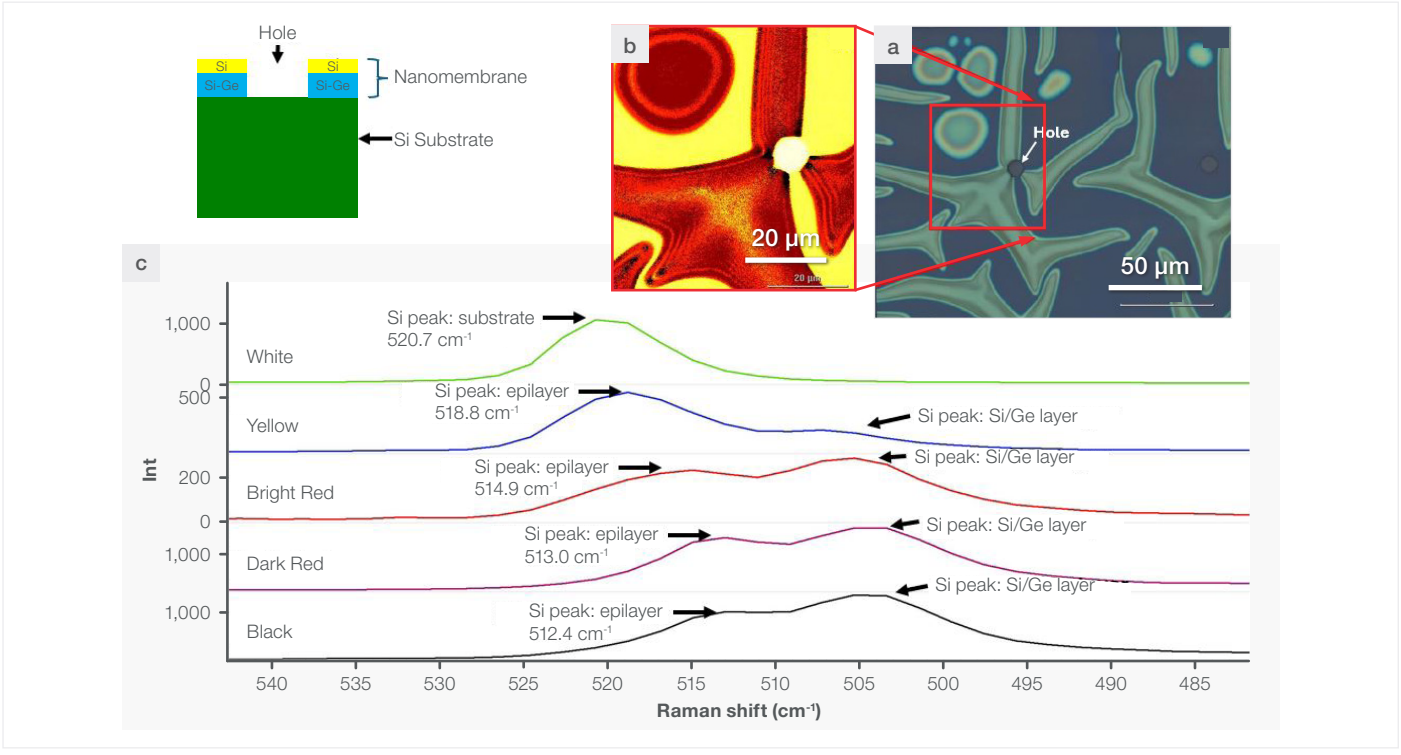

Figure 5. (a) Visual mosaic image of the silicon nanomembrane sample. (b) Raman peak position image based on the silicon peak of either the silicon substrate or the silicon epilayer. (c) Representative spectra from the colored areas in the Raman image (5b).

Figure 6 illustrates the application of Raman microscopy for imaging the stress distribution on the surface of a silicon wafer with LOCOS (local oxidation of the silicon) structures fabricated on the wafer. The LOCOS technique has been widely used to form silicon dioxide (SiO_2) in selected areas on a silicon wafer for lateral isolation between miniaturized active components. However, the isolation structures introduce significant local mechanical stress in silicon. This stress may cause dislocation and structural defects, resulting in decay in the performance and reliability of the active components.

Figure 6(a) shows the fragment of the LOCOS structure on a silicon wafer observed through a 100x (0.9 NA) metallurgical objective, while in Figure 6b a Raman spectral image is superimposed on the central part of the structure containing four SiO_2 insulating "islands". The Raman imaging data was acquired using a 532 nm laser for excitation (6 mW of the laser power at the sample), a 25 µm confocal pinhole and an image pixel size of 0.1 µm. The Raman image was generated as the position of the strong peak of silicon at ~520 cm^{-1} arising from the first order Raman transverse optical (TO) phonon mode. The typical Raman peaks retrieved from the red and blue areas of the Raman image, along with their positions and full widths at half maximum (FWHM), are shown in Figure 6d. The positions and FWHMs were rectified by curve-fitting the experimental peak profiles in Gaussian/ Lorentzian approximation. The shift to lower wavenumbers relative to 520 cm^{-1} (usually assigned to the position of the Raman peak in unstrained silicon) and the broadening of the peak from red to blue indicate tensile stress under the micro areas (~1 µm width) of the SiO_2 "islands" formed above and below the surface of the silicon wafer. The topographic profile of the fragment of the LOCOS structure with similar SiO_2 insulating "islands," obtained with the use of atomic force microscopy (AFM), is shown in Figure 6c. Since SiO_2 is transparent when using the 532 nm wavelength laser, the oxide does not result in a measurable contribution to the Raman spectrum, such that only the Raman peaks from the underlying silicon at the Si-SiO_2 interface are obtained.

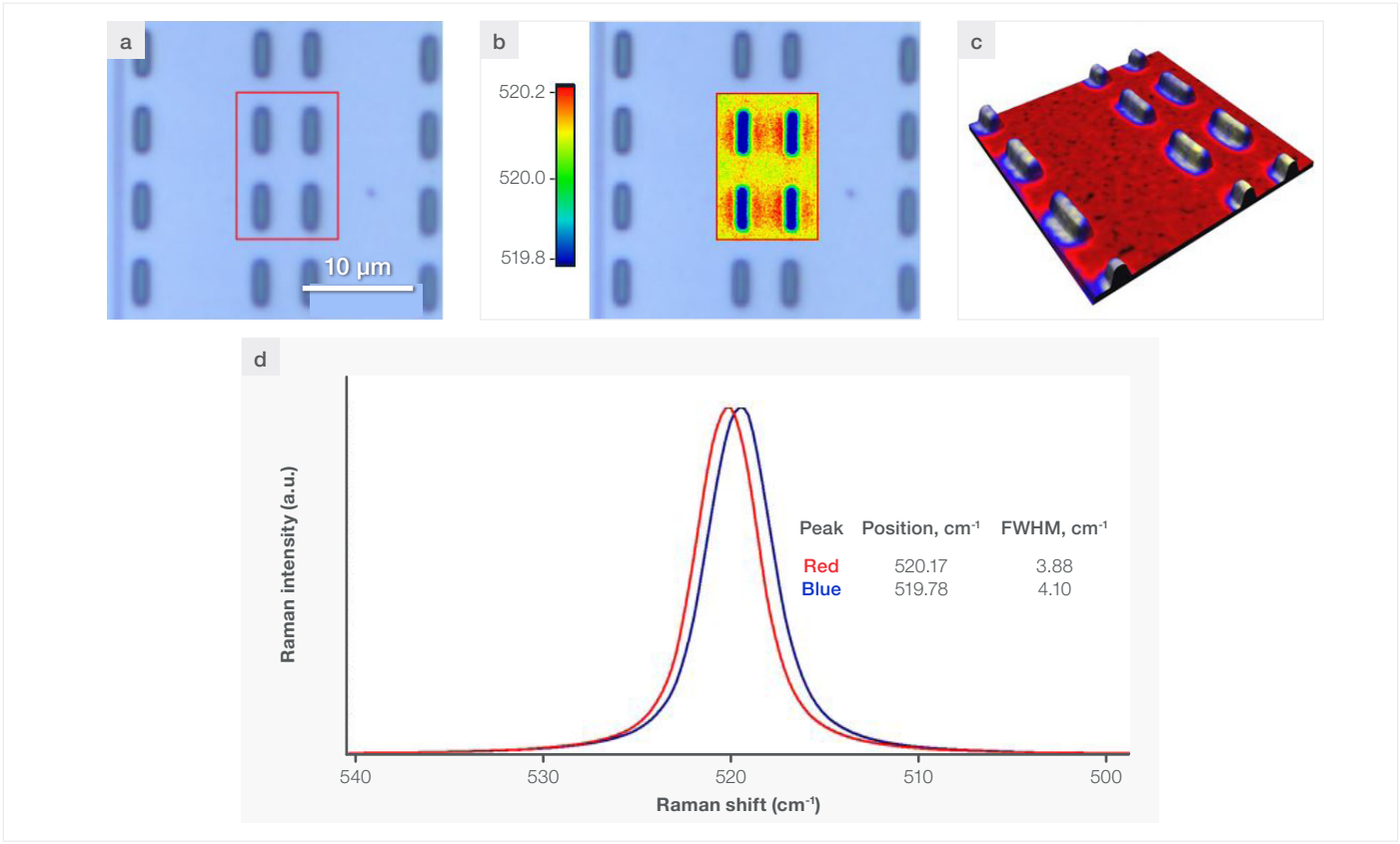

Figure 6. (a) Visual image of the LOCOS structure fabricated on the silicon wafer. (b) Raman image generated as the position of the first order TO phonon peak at ~ 520 cm^{-1} superimposed on the visual image. (c) Topographic profile of the LOCOS structure obtained using AFM. (d) The typical Raman peaks retrieved from the corresponding-colored areas of the Raman image (6b) and their major parameters.

Conclusion

The importance of silicon as a technologically significant material cannot be overstated. It has properties that make it useful in numerous different types of products. Raman micro-spectroscopy has proven itself an important tool for the assessment of molecular structure and physical states of silicon. Raman images provide a way to observe the spatial distribution of silicon and silicon-containing components, structural variations such as crystallinity, and physical effects such as strain. This note showed a few representative examples to illustrate some of the advantages offered by Raman microscopic analysis of silicon. The coverage is not intended to be comprehensive as there are numerous other areas where the Raman analysis of silicon is currently employed and other opportunities where it could be used. The Thermo Scientific DXR3 Raman Microscope and the Thermo Scientific DXR3xi Raman Imaging Microscope have both been shown to be excellent choices for the Raman analysis of silicon samples.

References

1. M.G. Mueller, M. Fornabaio, G. Zagar, A. Mortensen, Microscopic strength of silicon particles in aluminum-silicon alloy, *Acta Materialia* **2016**, 105, 165-175.
2. USDA Website *How is aluminum foil made? (usda.gov)*
3. Minjun Je, Dong-Yeob Han, Jaegeon Ryu, Soojin Park, Constructing Pure Si Anodes for Advanced Lithium Batteries, *Acc. Chem. Res* **2023**, 56, 2213-2224
4. V.A. Sethuraman, M.J. Chon, M. Shimshak, N. Van Winkle, P.R. Guduru, In situ measurement of biaxial modulus of Si anode for Li-ion batteries, *Electrochemistry Communications*, **2010**, 12, 1614-1617
5. Lee, P. S., Mangelinck, D., Pey, K. L., Shen, Z., Ding, J., Osipowicz, T., et al. Micro-Raman spectroscopy investigation of nickel silicides and nickel (platinum) silicides. *Electrochem. Solid-State Lett*, **2000**, 3(3), 153-155.
6. P. Chatterjee, Y. Pan, E.C. Stevens, T. Ma, H. Jiang, L.L. Dai, Controlled Morphology of Thin Film Silicon Integrated with Environmentally responsive Hydrogels, *Langmuir* **2013**, 29, 6495-6501
7. F. Cavallo, K.T. Turner, M.G. Lagally, Facile Fabrication of Ordered Crystalline-Semiconductor Microstructures on Compliant Substrates, *Adv. Funct. Mater.* **2014**, 24, 1730-1735.
8. Sample graciously provided by Dr. Francesca Cavallo while working with Professor Max G. Lagally in the Department of materials and Engineering, University of Wisconsin Madison.
9. Ingrid De Wolf, Micro-Raman spectroscopy to study local mechanical stress in silicon integrated circuits, *Semicond. Sci. Technol* **1996**, 11, 139-154.
10. V. Moroz, N. Strecker, X. Xu, L. Smith, I. Bork, Modeling the impact of stress on silicon processes and devices, *Materials Science in Semiconductor Processing*, **2003**, 6, 27-36.
11. L. Ma, W. Qiu, X. Fan, Stress/strain characterization in electronic packaging by micro-Raman spectroscopy: A review, *Microelectronics Reliability*, **2021**, 118, 114045.
12. Sample graciously provided by Dr. Jose R. Sanchez-Perez while working in Professor Max Lagally's group in the Department of Materials Science and Engineering at the University of Wisconsin Madison.

Learn more at **thermofisher.com/raman**